

# ADSORPTIVE REMOVAL OF $\text{Cu}^{2+}$ , $\text{Pb}^{2+}$ , AND $\text{Cr}^{6+}$ FROM PHARMACEUTICAL WASTEWATER USING GRAPHENE/RUTILE ( $\text{TiO}_2$ ) NANOCOMPOSITES

\*<sup>1</sup>John Tsado Mathew, <sup>2</sup>Inobeme Abel, <sup>3</sup>Elijah Yanda Shaba, <sup>1</sup>Musah Monday, <sup>1</sup>Yakubu Azeh, <sup>4</sup>Hassana Abubakar, <sup>3</sup>Aliyu Ibn Adam, <sup>1</sup>Muhammad Aishetu Ibrahim, <sup>1</sup>Hauwa Alfa Muhammad, <sup>1</sup>Ismail Haruna, <sup>1</sup>Umar Musa Tanko, <sup>5</sup>Aliyu Mohammed Sakpe, <sup>6</sup>Solomon Papa Yisa, <sup>7</sup>Ismaila Aliyu Oga, <sup>7</sup>Etsuyankpa Muhammad Bini, <sup>7</sup>Musa Safiyanku Tanko, <sup>1</sup>Amos Mamman

<sup>1</sup>Department of Chemistry, Ibrahim Badamasi Babangida University, Lapai, Nigeria

<sup>2</sup>Department of Chemistry, Edo State University, Uzairue, Nigeria

<sup>3</sup>Department of Chemistry, Federal University of Technology, Minna, Nigeria

<sup>4</sup>Department of Biochemistry and Biotechnology, Ibrahim Badamasi Babangida University, Lapai, Niger State, Nigeria

<sup>5</sup>Department of Basic Sciences, Niger State College of Agriculture, Mokwa, Nigeria

<sup>6</sup>Pre-ND Sciences, Niger State College of Agriculture, Mokwa, Nigeria

<sup>7</sup>Department of Chemistry, Federal University of Lafia, Nasarawa State, Nigeria

\*Corresponding Author Email Address: [jmathew@ibbu.edu.ng](mailto:jmathew@ibbu.edu.ng)

## ABSTRACT

Demand for safe drinking water is becoming a challenging issue, having been greatly influenced by human activities and the growing world population. Nanotechnology offers a promising solution through the applications of nanomaterials. This research investigated the equilibrium adsorption mechanism and thermodynamics of the removal of Copper ( $\text{Cu}(\text{II})$ ), Lead ( $\text{Pb}(\text{II})$ ), and Chromium ( $\text{Cr}(\text{VI})$ ) from pharmaceutical wastewater onto the synthesized graphene/ $\text{TiO}_2$  nanocomposites produced from Palm kernel shell and Titanium dioxide as a low-cost adsorbent. The synthesized graphene/ $\text{TiO}_2$  nanocomposites were characterized using Scanning Electron Microscope (SEM), Energy Dispersive X-rays (EDX), X-ray Diffraction, UV-Visible absorbance, and Fourier Transform Infrared (FTIR) Spectrophotometry before adsorption of metal ions (Copper, Lead, and Chromium). The result of batch experiments indicates that 99%, 60 % and 20 % of  $\text{Cu}(\text{II})$ ,  $\text{Pb}(\text{II})$ , and  $\text{Cr}(\text{VI})$  were removed using graphene/ $\text{TiO}_2$  nanocomposites under the optimal conditions of contact time (25 min), temperature ( $40^\circ\text{C}$ ), and adsorbent dosage (0.12 g). The adsorption kinetics showed that the adsorption of  $\text{Cu}(\text{II})$ ,  $\text{Pb}(\text{II})$ , and  $\text{Cr}(\text{VI})$  from the pharmaceutical wastewater fits better into the pseudo-second order for all the heavy metals removed. The recyclability studies indicate that the graphene/ $\text{TiO}_2$  nanocomposites were stable and maintained 75 % adsorption removal after four consecutive recyclability studies. The findings from this research indicate that graphene/ $\text{TiO}_2$  nanocomposites is a potential adsorbent that can be used to remove heavy metals from pharmaceutical wastewater and any other related industries.

**Keywords:** Heavy, Nanocomposites, Metals, Pharmaceutical, Wastewater

## INTRODUCTION

Pharmaceutical wastewater is a widespread environmental concern due to its complex composition and high concentration of toxic contaminants, including heavy metals such as lead ( $\text{Pb}$ ), cadmium ( $\text{Cd}$ ), and chromium ( $\text{Cr}$ ) (Madesh *et al.* 2024). The metals, typically brought into play with the synthesis and processing of pharmaceutical compounds, are of serious concern to human health and the environment due to their toxicity, lack of

biodegradability, and potential for bioaccumulation (Edo *et al.* 2024). Conventional wastewater treatment techniques such as chemical precipitation, ion exchange, and membrane filtration are often limited by high operation cost, sludge generation, and low metal removal rates, particularly at low metal levels (Mathew *et al.* 2024a). By way of reaction, there is a growing demand for affordable, sustainable, and effective treatment technologies specifically tailored for heavy metal removal from pharmaceutical wastewaters (Adetunji *et al.* 2023; Mathew *et al.* 2023a).

Among the recent technologies, adsorption has been extremely popular due to its ease, low energy requirement, and high efficiency, especially when using innovative adsorbent materials. Nanomaterials with high surface areas and modifiable surface chemistry have been reported to be effective for the adsorption of metal ions from aqueous solutions (Etsuyankpa *et al.* 2024; Naz *et al.* 2025). Graphene, which is a two-dimensional material made of carbon, has outstanding physicochemical characteristics such as a vast surface area, high mechanical strength, and availability of  $\pi$ -electrons, and so graphene is an excellent adsorbent (Adetunji *et al.* 2022; Bhowmik *et al.* 2025). When graphene is mixed with metal oxides such as titanium dioxide ( $\text{TiO}_2$ ), especially in rutile form, the obtained nanocomposite enjoys the positive features of both: the high conductivity and surface activity of graphene and the stability and photocatalytic activity of  $\text{TiO}_2$ . The interaction of these materials is enhanced in terms of adsorption capability and selectivity towards heavy metals (Inobeme *et al.* 2024; He *et al.* 2025).

This research focuses on the development and evaluation of graphene/rutile  $\text{TiO}_2$  nanocomposites for the adsorptive removal of specific heavy metals from pharmaceutical wastewater. The nanocomposites are synthesized and characterized to determine their structure, morphology, and surface characteristics. Batch adsorption experiments are conducted to investigate the effect of the significant parameters such as contact time, adsorbent dose, pH, FTIR and temperature. Data are analyzed in terms of adsorption isotherms, thermodynamics and kinetic models to determine the mechanism of metal adsorption. The primary objective is to provide a comprehensive understanding of the

promise of graphene/TiO<sub>2</sub> nanocomposites as a scalable, feasible, and eco-friendly solution for the remediation of heavy metal-polluted pharmaceutical wastewater in the context of environmental protection and sustainable industrial processes.

## MATERIALS AND METHODS

All chemicals used in this study were of analytical grade and used without further purification. Graphite oxide was produced from palm kernel shell, titanium(IV) isopropoxide (TTIP), nitric acid (HNO<sub>3</sub>), sulfuric acid (H<sub>2</sub>SO<sub>4</sub>), potassium permanganate (KMnO<sub>4</sub>), hydrogen peroxide (H<sub>2</sub>O<sub>2</sub>, 30%), and hydrochloric acid (HCl) were purchased from Sigma-Aldrich. Deionized (DI) water was used throughout the experiments. Pharmaceutical wastewater was collected from the effluent discharge point of a local pharmaceutical manufacturing facility. The samples were filtered to remove suspended solids and stored at 4 °C prior to use.

### Synthesis of Graphene Oxide (GO)

Graphene oxide (GO) was synthesized using a modified Hummers' method. For a moment, 3 g of graphite powder was added to a mixture of 69 cm<sup>3</sup> of concentrated H<sub>2</sub>SO<sub>4</sub> and 1.5 g of NaNO<sub>3</sub> under ice bath conditions. While stirring, 9 g of KMnO<sub>4</sub> was gradually added to the suspension, keeping the temperature below 20 °C. The mixture was then stirred at 35 °C for 2 hours, followed by slow addition of 138 cm<sup>3</sup> of deionized water. After 30 minutes, 420 cm<sup>3</sup> of deionized water and 3 cm<sup>3</sup> of H<sub>2</sub>O<sub>2</sub> were added to stop the reaction. The resulting product was washed with HCl and DI water repeatedly, then dried at 60 °C to obtain GO powder.

### Synthesis of Graphene/Rutile TiO<sub>2</sub> Nanocomposites

The graphene/rutile TiO<sub>2</sub> nanocomposite was synthesized via a sol-gel-assisted hydrothermal method. In a typical procedure, 1 g of GO was dispersed in 100 cm<sup>3</sup> of ethanol and ultrasonicated for 1 hour. Separately, 10 cm<sup>3</sup> of TTIP was added dropwise to 50 cm<sup>3</sup> of ethanol under stirring to form the precursor solution. The two solutions were mixed and stirred for 2 hours, followed by hydrothermal treatment in a Teflon-lined autoclave at 180 °C for 12 hours. The resulting precipitate was filtered, washed, and calcined at 500 °C for 2 hours to obtain the graphene/rutile TiO<sub>2</sub> nanocomposite (Idris *et al.* 2024; Musa *et al.* 2024).

### Characterization

The nanocomposites were characterized to confirm their structural

and surface properties. X-ray diffraction (XRD) was used to identify the crystalline phases. Scanning electron microscopy (SEM) and transmission electron microscopy (TEM) provided morphological information. Fourier-transform infrared spectroscopy (FTIR) was used to identify functional groups. Brunauer–Emmett–Teller (BET) analysis was conducted to determine surface area and pore size distribution. UV–Vis spectroscopy was employed to evaluate optical properties (Muhammad *et al.* 2024).

### Batch Adsorption Experiments

Batch adsorption studies were conducted to evaluate the removal efficiency of Cu<sup>2+</sup>, Pb<sup>2+</sup>, and Cr<sup>6+</sup>. In each experiment, 100 cm<sup>3</sup> of synthetic or real wastewater containing known concentrations of the target metal ions was mixed with a fixed dose of the nanocomposite in a 250 cm<sup>3</sup> Erlenmeyer flask. The effects of key operational parameters such as pH (2–8), contact time (10–180 minutes), initial metal concentration (10–100 mg/L), and adsorbent dosage (0.1–1.0 g/L) were investigated (Mathew *et al.* 2024b). The pH was adjusted 9 using 0.1 M HCl or NaOH. Samples were agitated in a thermostatic shaker at 150 rpm and 25 °C. After the predetermined contact time, samples were filtered, and the residual metal ion concentrations were measured using atomic absorption spectroscopy (AAS) (Mathew, *et al.* 2023b).

### Adsorption Isotherm and Kinetic Modeling

To understand the adsorption mechanism, the experimental data were fitted to the Langmuir and the Freundlich isotherm models. Kinetic behavior was analyzed using pseudo-first-order and pseudo-second-order models. Thermodynamic parameters such as Gibbs free energy (ΔG°), enthalpy (ΔH°), and entropy (ΔS°) were also calculated to assess the nature of adsorption. The isothermal experimental data were evaluated using the Langmuir and Freundlich adsorption models, as described by Mathew *et al.* (2024c).

## RESULTS AND DISCUSSION

### SEM analysis of Graphene/TiO<sub>2</sub>-Rutile (G/TiO<sub>2</sub>-R) nanocomposites

Figure 1 shows that the morphology of the G/TiO<sub>2</sub>-R nanocomposites synthesized was spherical and had small particles with less agglomeration. The majority of the particles seen are due to the high temperature of calcination, and the use of gelatin provides long-term stability for nanoparticles.

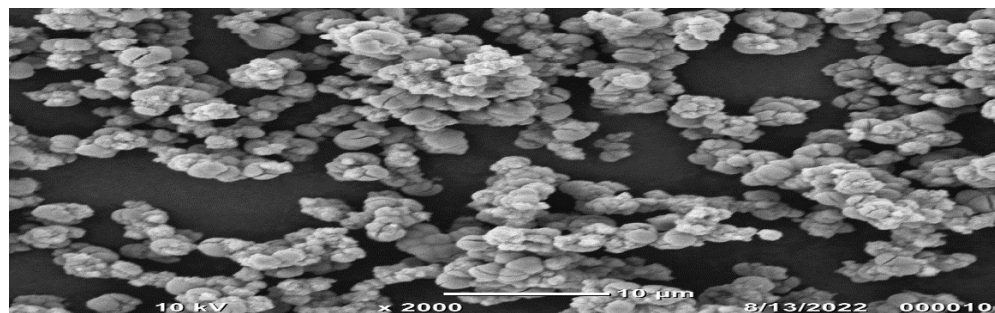


Figure 1: SEM image of G/TiO<sub>2</sub>-R NCs

### Energy dispersive spectroscopy (EDX) analysis

Energy dispersive spectroscopy from the graph below revealed the stoichiometric proportion of Ti, O, Cl and C elements (Mousavi, and

Rahmani, 2025). Here it is seen that Ti and O are major elements with % atomic weight of 41.92 and 36.85. It shows the signal that confirms the ratio of Ti:O=2:1 .

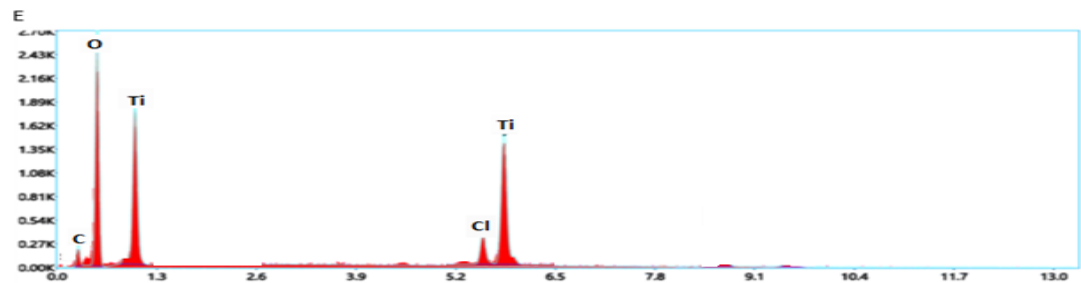


Figure 2: EDX image of G/TiO<sub>2</sub> RNCs

Table 1: Percentage compositions of EDX

C Element	%Weight
O	13.98
Cl	2.50
Ti	33.82
Ti	49.70

**XRD analysis**

X-ray diffraction is an analytical technique used to characterize crystalline phases. The interaction of the incident rays with the sample produces constructive interference when conditions satisfy Bragg's law:  $n\lambda = 2d\sin\theta$ , where  $n$  is an integer,  $\lambda$  is the wavelength of the x-ray,  $d$  is the interplanar spacing generating the diffraction, and  $\theta$  is the diffraction angle (Kayadurmus *et al.*, 2025). Figure 3 below shows a crystalline 3D phase. This is different from the spherical shape you obtained, structural periodicity, and diffraction sharp maxima, and a constructive interference which occurs due to the path difference of the scattered wave from consecutive layers of atoms, is a multiple of the wavelength of the x-ray, which satisfies Bragg's law. The full width at half maximum (FWHM), which determines the grain size and residual strain, is at  $40\text{--}45^\circ(2\theta)$ .

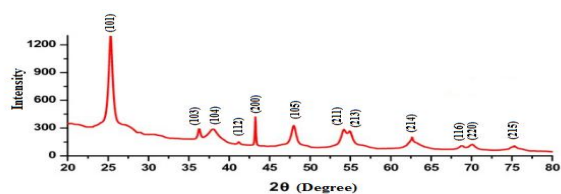


Figure 3: XRD Spectrum of G/TiO<sub>2</sub>-R Nanocomposite

Table 2: Surface Area, and Total Pore Volume of Graphene (G) and Rutile Titanium oxide G/TiO<sub>2</sub>-R nanocomposites

Sample	BET Surface area(m <sup>2</sup> /g)	Total Pore Volume (cm <sup>3</sup> /g)
TiO <sub>2</sub> -R	6.031	0.492

From Table 2 above, it shows that TiO<sub>2</sub>-R has the highest surface area and total pore volume compared to G. By this study, it implies that TiO<sub>2</sub>-R has its activity directly proportional to its concentration from Langmuir and the isotherm theory of Brunaur Emmett Teller (BET). Graphene will have less interaction with the adsorption capacity of particles due to the amount of temperature, pressure, and strength being lower.

**UV-Visible spectrum analysis**

Figure 4 of the UV-visible spectrum analysis shows a maximum peak at 490nm, which is observed to have a chromophore of

nitroso and transition  $n\text{--}\pi^*$  at the excited level, due to the presence of acid. The wavelengths absorb the colour of visible light as blue and reflect the colour as yellow.

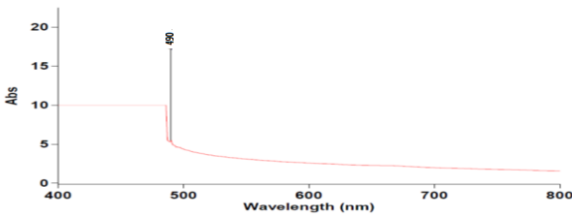


Figure 4: UV-Visible spectrum of G/TiO<sub>2</sub>-R NCs

**FTIR spectrum analysis**

The functional group of G/TiO<sub>2</sub>-R obtained from FTIR spectrum analysis shows the band at 3208, which indicates a hydroxyl group. At 2128 cm<sup>-1</sup>, it revealed C $\equiv$ C terminal alkyne. However, 1636 cm<sup>-1</sup> shows the presence of unsaturated C=C aromatic compounds. The band at 1084 cm<sup>-1</sup> revealed OH stretch, and 1043 cm<sup>-1</sup> shows cyclohexane ring vibrations.

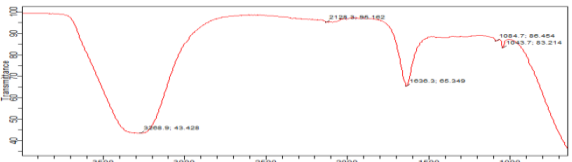
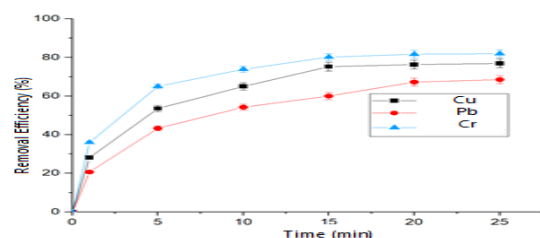


Figure 5: FTIR spectrum of G/TiO<sub>2</sub>-R NCs

Table 3: FTIR Band assignment

Wavelength Cm <sup>-1</sup>	Band assignment/functional group	References
3208	Hydroxyl group	Mohammad <i>et al.</i> , 2025
2128	C $\equiv$ C	Mohammad <i>et al.</i> , 2025
1636	C=C	Lazaridou <i>et al.</i> , 2025
1043	Cyclohexane ring	Sisti <i>et al.</i> , 2025

### Effect of contact time



**Figure 6:** Effect of contact time

The effect of contact time on the rate of removal of Cr, Cu and Pb by adding synthesized G/TiO<sub>2</sub>-R to an aqueous solution. The removal efficiency of the toxic metals starts earlier. At 15mins, 80% of Cr was removed. At that same 15mins, Pb and Cu was removed at a varying percentage of 58% and 78% respectively which shows that Cr has the highest removal efficiency however, remains constant from 20mins to 25mins.

### Effect of adsorbent dose

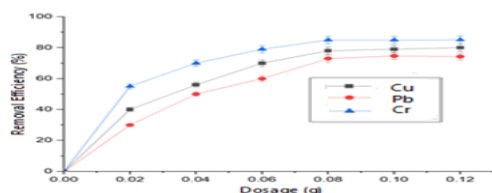


**Figure 7:** effect of adsorbent dose

Synthesized G/TiO<sub>2</sub>-R is a potential candidate for removing toxic metals from wastewater, which was added to an aqueous solution. According to the figure above, Cu, Cr, and Pb start with the same dosage, but at 0.08g, Cr has the highest removal efficiency of 85% and falls a bit to 80% at a dosage of 0.10g and remains at that to 0.12g. The toxic contaminants, Cu, and Pb were absorbed at 78% and 76% respectively (Moeng *et al.*, 2022). The statement implies that G/TiO<sub>2</sub>-R shows selective adsorption, with Cr removed most efficiently, while Cu and Pb remain slightly lower, demonstrating the material's potential for targeted heavy metal wastewater treatment.

### Effect of adsorption temperature

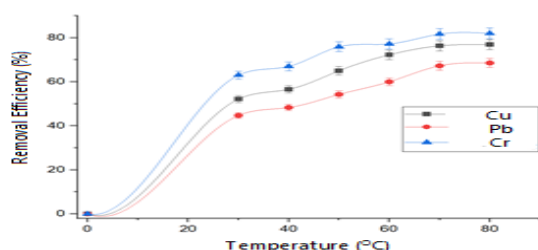


**Figure 8:** effect of adsorption temperature

The temperature influences the heavy metal ions adsorption. Adsorption removal efficiency percentage starts immediately from 0°C for Cr after the addition of G/TiO<sub>2</sub>-R to an aqueous solution. The removal efficiency rises and falls gradually as the adsorption temperature increases, varying for Cr, Cu, and Pb. The maximum

removal efficiency is at 80% which is for Cr with an adsorption temperature of 80 °C.

**Table 4:** Thermodynamic parameters for the metal ions

Parameter	$\Delta H$ (kJ/mol)	$\Delta S$ (kJ/mol)	$\Delta G$ (kJ/mol)			
			303 K	313 K	323 K	333 K
Cu	27.209	67.25	6.97	6.26	5.70	4.50
Pb	2.911	5.040	1.47	1.44	1.42	1.43
Cr	9.932	23.59	2.60	2.37	2.14	2.05

Thermodynamic parameters of adsorption from solutions provide a great deal of information concerning the type and mechanism of the adsorption process. A negative Gibbs free energy ( $\Delta G^\circ$ ) value indicates the feasibility and spontaneous nature of the adsorption process. The relationship of  $\Delta G^\circ$  to enthalpy change ( $\Delta H^\circ$ ) and entropy change ( $\Delta S^\circ$ ) of adsorption is expressed as  $\Delta G^\circ = \Delta H^\circ - T\Delta S^\circ$ . The positive value of  $\Delta H^\circ$  indicates that the adsorption is an endothermic process, while the positive value of  $\Delta S^\circ$  reflects the increased randomness at the solution interface.

From Table 4, the  $\Delta G^\circ$  value indicates that the adsorption process is non-spontaneous for Cr, Cu, and Pb. The positive value of  $\Delta H^\circ$  indicates that the sorption is an endothermic process, while  $\Delta S^\circ$  reflects the increase in randomness at the solution interface, and the energy of adsorption, according to the Langmuir equation, remains constant (Wang and Zhang, 2021).

**Table 5:** Pseudo-first order and Pseudo-second order parameters for the adsorption of copper, lead, and chromium ions

Parameter	Pseudo first order				Pseudo second order		
	$R^2$	$Q_e$	$K_1$	$Q_{exp}$	$R^2$	$Q_e$	$K_2$
Cu	0.170	1.2	0.5	1.6	0.9	1.6	0.1
Pb	0.616	8.7	0.6	1.5	0.9	0.3	0.6
Cr	0.612	5.3	0.6	1.6	0.4	0.7	0.3

Both pseudo-first and second-order adsorption were used to describe the sorption of heavy metals. In both models, all the steps of adsorption such as internal diffusion, external diffusion and adsorption are lumped together and it is assumed that the difference between the average solid phase concentration and the equilibrium concentration is the driving force for adsorption and that the overall adsorption rate is proportional to either the driving force (as in the pseudo first order) or the square of the driving force (as in the pseudo second order). According to the correlation coefficients, both models give satisfactory fits, which vary a lot been it that, for the pseudo first order is higher. But the calculated adsorption amount at equilibrium shows a difference comparison for the pseudo-second order to be a fitting model for Cu, Cr and Pb.



## Conclusion

TiO<sub>2</sub>-R nanoparticles were prepared by the sol-gel method, which is a current, simple, cost-effective, and environmentally friendly synthesis for structural and morphological characterization using different techniques. The result revealed the agglomeration, stoichiometric, chromophore, and chemical composition. Also, results from different techniques confirmed the authenticity of G/TiO<sub>2</sub>-R in the application of wastewater treatment to remove various contaminants for safe use.

## REFERENCES

- Adetunji, C. O., Ogundolie, F. A., Mathew, J. T., Inobeme, A., Olotu, T., Olaniyan, O. T., Ijadeniyi, O. A., Ajiboye, M. D., Ajayi, O. O., Dauda, W., Ghazanfar, S. and Adetunji, J. B. (2022). Graphene-based nanomaterials for targeted drug delivery and tissue engineering. In a book: Novel Platforms for Drug Delivery Applications. Elsevier Ltd. 277 – 288. doi: <https://doi.org/10.1016/B978-0-323-91376-8.00014-8>
- Adetunji, C. O., Olaniyan, O. T., Inobeme, A., Adeyomoye, O., Mathew, J. T. and Akinbo, O. (2023). Recent Advances in the Characterization and Application of Graphene in the Food Industry. In book: Sensing and Artificial Intelligence Solutions for Food Manufacturing. CRC Press, 153-164. doi: 10.1201/9781003207955-11.
- Bhowmik, S., Mufeed, M., Phukan, S. J., Sarkar, S., Goswami, S., Khan, K. A., ... & Saha, M. (2025). Contemporary Progress on Graphene/Graphene Derivatives-Based Adsorbents and Photocatalysts for the Eradication of Organic Toxins: An Updated Overview. *Chemistry–An Asian Journal*, e00628.
- Edo, G. I., Samuel, P. O., Oloni, G. O., Ezekiel, G. O., Ikpekor, V. O., Obasohan, P., ... & Agbo, J. J. (2024). Environmental persistence, bioaccumulation, and ecotoxicology of heavy metals. *Chemistry and Ecology*, 40(3), 322-349.
- Etsuyankpa, M. B., Augustine, A. U., Musa, S. T., Mathew, J. T., Ismail, H., Salihu, A. M., Mamman, A (2024). An Overview of Wastewater Characteristics, Treatment and Disposal: A Review. *Journal of Applied Science and Environmental Management*, 28 (5) 1553-1572. Doi: <https://dx.doi.org/10.4314/jasem.v28i5.28>.
- He, Y., Zhang, L., Li, X., Jin, L., & Huang, X. (2025). Synergistic CoS<sub>2</sub>-SnS<sub>3</sub> heterojunction in N-doped carbon for enhanced and selective heavy metal removal via capacitive deionization. *Desalination*, 608, 118823.
- Idris A. Y., Elele U. U. and Mathew, J. T. (2024). Preparation and characterization of MoO<sub>3</sub> nanoparticles for the photocatalytic degradation of dyeing wastewater. *Science World Journal Vol.* 19(4), 1006-1011. <https://dx.doi.org/10.4314/swj.v19i4.14>
- Inobeme, A., Mathew, J.T., Adetunji, C.O., Agbugui, M.O., Osarenren, E.J., Oti, C., Ngonso, B.F., Inobeme, J., Oyedolapo, M.B., Bernard, E. & Jibrin, N.A. (2024). Biocomposites with graphene derivatives. In book: Advances in Biocomposites and their Applications, Elsevier Inc., 149-166. DOI: 10.1016/B978-0-443-19074-2.00005-8
- Kayadurmus, H. M., Ayran, M., Goktug, S., Gunduz, O., & Dogan, C. (2025). Spectroscopic characterization of biomaterials for tissue engineering applications. *Biomedical Materials & Devices*, 3(1), 153-169.
- Lazaridou, M., Moroni, S., Klonos, P., Kyritsis, A., Bikiaris, D. N., & Lamprou, D. A. (2025). 3D-printed hydrogels based on amphiphilic chitosan derivative loaded with levofloxacin for wound healing applications. *International Journal of Polymeric Materials and Polymeric Biomaterials*, 74(2), 67-84.
- Madesh, S., Sudhakaran, G., Meenatchi, R., Guru, A., & Arockiaraj, J. (2024). Interconnected environmental challenges: heavy metal–drug interactions and their impacts on ecosystems. *Drug and Chemical Toxicology*, 47(6), 1282-1299.
- Mathew, J. T., Inobeme, A., Musah, M., Azeh, Y., Abdullahi, A., Shaba E. Y., Salihu, A. M., Muhammad, E. B., Josiah, J. G., Jibrin, N. A., Ismail, H., Muhammad, A. I., Maurice, J., Mamman, A. & Ndamitso, M. M. (2024)a. A Critical Review of Green Approach on Wastewater Treatment Strategies. . *Journal of Applied Science and Environmental Management*, 28(2), 363-391. doi: <https://dx.doi.org/10.4314/jasem.v28i2.9>
- Mathew, J. T., Musah, M., Azeh, Y. & Muhammed, M. (2024)b. Development of Fe<sub>3</sub>O<sub>4</sub> Nanoparticles for the Removal of Some Toxic Metals from Pharmaceutical Wastewater. *Caliphate Journal of Science & Technology (CaJoST)*, 6(1), 26-34. Doi: <https://dx.doi.org/10.4314/cajost.v6i1.4>
- Mathew, J. T., Musah, M., Azeh, Y. and Musa, M. (2024)c. Removal of Some Toxic Metals from Pharmaceutical Wastewater Using Geopolymer/Fe<sub>3</sub>O<sub>4</sub>/ZnO nanocomposite: Isotherm, Kinetics and Thermodynamic Studies. *Confluence University Journal of Science and Technology*, 1(1): 50-58. Doi: 10.5455/CUJOSTECH.240706
- Mathew, J. T., Musah, M., Azeh, Y. & Muhammed, M. (2023)a. Adsorptive Removal of Selected Toxic Metals from Pharmaceutical Wastewater using Fe<sub>3</sub>O<sub>4</sub>/ZnO Nanocomposite, *Dutse Journal of Pure and Applied Sciences*, 9(4a), 236- 248. <https://dx.doi.org/10.4314/dujopas.v9i4a.22>
- Mathew, J. T., Musah, M., Azeh, Y. & Muhammed, M. (2023)b. Kinetic Study of Heavy Metals Removal from Pharmaceutical Wastewater Using Geopolymer/Fe<sub>3</sub>O<sub>4</sub> Nanocomposite. *Bima Journal of Science and Technology*, 7(4), 152- 163. Doi: 10.56892/bima.v7i4.539.
- Moeng, M. M., Malan, F. P., Lotz, S., & Bezuidenhout, D. I. (2022). Fischer carbene complexes of cobalt (I): Synthesis and structure. *Journal of Molecular Structure*, 1252, 132093.
- Mohammad, F., Azizi, N., Mirjafary, Z., & Mokhtari, J. (2025). Catalytic alkenylation of oxindoles using a silica-supported deep eutectic solvent. *Journal of Molecular Liquids*, 128467.
- Mousavi, S. M., & Rahmani, M. B. (2025). Enhanced Photocatalytic Performance of Semicrystalline Cl-Doped PPy@ TiO<sub>2</sub> Nanocomposites for MB Degradation. *Polymers for Advanced Technologies*, 36(8), e70312.
- Muhammad, M. S., Musah, M. and Mathew, J. T. (2024). Preparation and Characterization of Activated Carbon from Africa Star Apple (*Chrysophyllum albidum*) Seed

- Shell. FUDMA Journal of Sciences (FJS), 8(3), 194-199. DOI: <https://doi.org/10.33003/fjs-2024-0803-2485>
- Musa A. V., Musah, M. and Mathew, J. T. (2024). Production and characterization of Zeolite-A nanoparticles for the treatment of pharmaceutical wastewater. *Science World Journal* Vol. 19(4), 987-993. <https://dx.doi.org/10.4314/swj.v19i4.11>
- Naz, H., Khalid, Z., Arif, S., Sattar, A., Ahmed, M. N., & Waseem, M. (2025). High removal efficiency of arsenite from aqueous solution by cobalt ferrite functionalized sawdust driven activated carbon. *Inorganic Chemistry Communications*, 178, 114615.
- Sisti, S., Ioele, F., Scarchilli, F., Laparelli, S., Galeotti, M., Hosseinzadeh, O., ... & Bietti, M. (2025). Hydrogen Atom Transfer-Based C (sp<sup>3</sup>)–H Bond Oxygenation of Lactams and Cycloalkenes: The Influence of Ring Size on Reactivity and Site Selectivity. *The Journal of Organic Chemistry*, 90(15), 5195-5205.
- Wang, J., & Zhang, W. (2021). Evaluating the adsorption of Shanghai silty clay to Cd (II), Pb (II), As (V), and Cr (VI): Kinetic, equilibrium, and thermodynamic studies. *Environmental monitoring and assessment*, 193(3), 131.